Available online at www.sciencedirect.com

ScienceDirect

Energy Procedia 68 (2015) 87 – 96

Energy Procedia

2nd International Conference on Sustainable Energy Engineering and Application, ICSEEA 2014

The effect of plate spacing in plate heat exchanger design as a condenser in organic Rankine cycle for low temperature heat source

Nur Rohmah[a,*], Ghalya Pikra[a], Andri Joko Purwanto[a], Rakhmad Indra Pramana[a]

[a]*Research Centre for Electrical Power and Mechatronics – Indonesian Institute of Science*
Komplek LIPI, Jl. Sangkuriang, Bandung 40135, Indonesia

Abstract

Plate spacing is one of variable that influences plate heat exchanger (PHE) design as a condenser in Organic Rankine Cycle (ORC) system. The rises of plate spacing have effects to channel cross sectional area, channel velocity, equivalent diameter, and Reynold number at hot and cold fluid sides in PHE. Those parameters affect the total heat transfer area and total pressure drop that influence the PHE condenser performance. This paper investigated the detail effect of the plate spacing increments in the final total heat transfer area and total pressure drop design result. The plate spacing in design calculation method is varied and the other independent variables are assumed to be constant. The design was conducted by calculating condenser capacity at both sides and both zones, estimating overall heat transfer coefficient, and calculating heat transfer area and plate film coefficient. Analysis continued by calculating overall heat transfer coefficient that has small percent of error with the estimated overall heat transfer coefficient, calculating pressure drop, total plate number and total heat transfer area. The result of calculation shows that the rises of plate spacing increase the total heat transfer area and decrease the cold and hot fluid total pressure drop. The rises of plate spacing increase channel cross sectional area and equivalent diameter, and decrease channel velocity and Reynold number at zone 1 (without phase change) and zone 2 (with phase change). Therefore, the increment of heat transfer areas is unpreferable and the decrement of pressure drops is preferable.

Peer-review under responsibility of Scientific Committee of ICSEEA 2014

Keywords: organic Rankine cycle (ORC); condenser; plate heat exchanger (PHE); plate spacing

* Corresponding author. Tel.: +62-22-2503055; fax: +62-22-2504773.
E-mail address: nur.rohmah@lipi.go.id

Peer-review under responsibility of Scientific Committee of ICSEEA 2014
doi:10.1016/j.egypro.2015.03.236

1. Introduction

Utilization of low temperature heat source into electricity has been developed in the world. This is done to reduce the dependence and the depletion of fossil fuel availability. Organic Rankine Cycle (ORC) is a system that can generate electricity at a low temperature heat source. ORC systems with low temperature heat source can provide excellent performance compared with other technologies [1-4]. ORC is a system that is flexible, safe and low maintenance costs [5-7]. ORC is a mature energy conversion technology and has been carried out in last two decades as extensive research [8]. Thermal efficiency ORC system was varies, from 0.02 to 0.11 [9, 10]. Design of heat exchangers in ORC, such as evaporator and condenser has a significant effect on the overall system performance [11]. Therefore, it is necessary to design for heat exchangers according to the capacity required to produce a good system performance.

Condenser as part of the heat exchanger is the component that serves to condense the steam from the turbine expansion to be pumped back to the evaporator. Design of condenser with PHE type is different from shell and tube type. PHE condenser needs to be designed in accordance with the required specifications, so that it can obtain good performance. Condenser dimensions and materials is an important part to get a good condensation process. Several studies have been conducted by researchers to get a good PHE specification. Wang et al. [12] presented a design method for PHEs with and without pressure drop specifications. Full utilization of allowable pressure drop was taken as the design objective, in the case of design with pressure drop specification. In the case of no pressure drop specification, allowable pressure drops were determined through economical optimization. Zhu et al. [13] discussed the integrated optimal design of the materials, placement, size and flow rate of a plate heat exchanger. By optimization, with a consequent reduction in cost, the PHE was effectively smaller than the real example given. Jiang Feng et.al [11] presented multi-objective optimization design of the PHE. The results show that a Pareto optimal point curve is obtained, which shows that a decrease in total heat transfer surface area of a condenser can increase the pressure drop through the condenser. Karellas et.al [14] investigated the influence of the ORC parameters on the heat exchanger design for supercritical condition. The analysis result was suggested an accurate method for supercritical heat exchangers' calculations and dimensioning and provides a very useful tool for future research on this field.

This paper will discuss the design of the condenser type of PHE for ORC systems with low temperature heat source. Design analysis done by plate spacing variations, in order to have the best specifications in accordance with the design, so that the system can produce a good performance.

2. Methodology

Plate heat exchanger (PHE) design as a condenser is divided into hot and cold side. Each side is divided into zone 1 (without phase change) and zone 2 (with phase changes). Fig. 1 and Fig. 2 show flow arrangement and plate arrangement of PHE. The design method flow chart to get PHE dimension that can be utilized as condenser of the operating condition in Table 1 is detailed in Fig. 3.

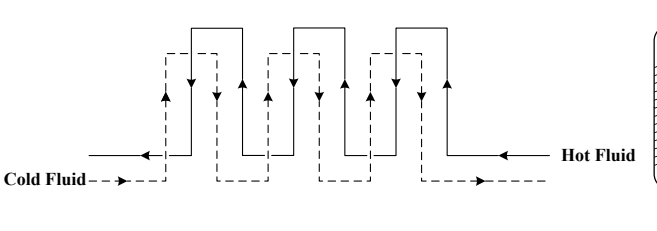

Fig. 1. Flow arrangement of PHE with 1-1 counter-current series [15].

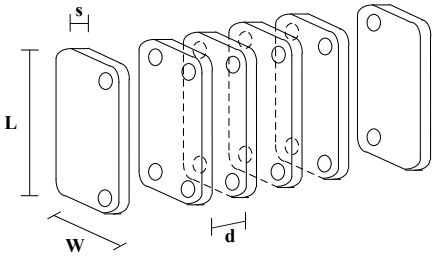

Fig. 2. Plate arrangement of PHE.

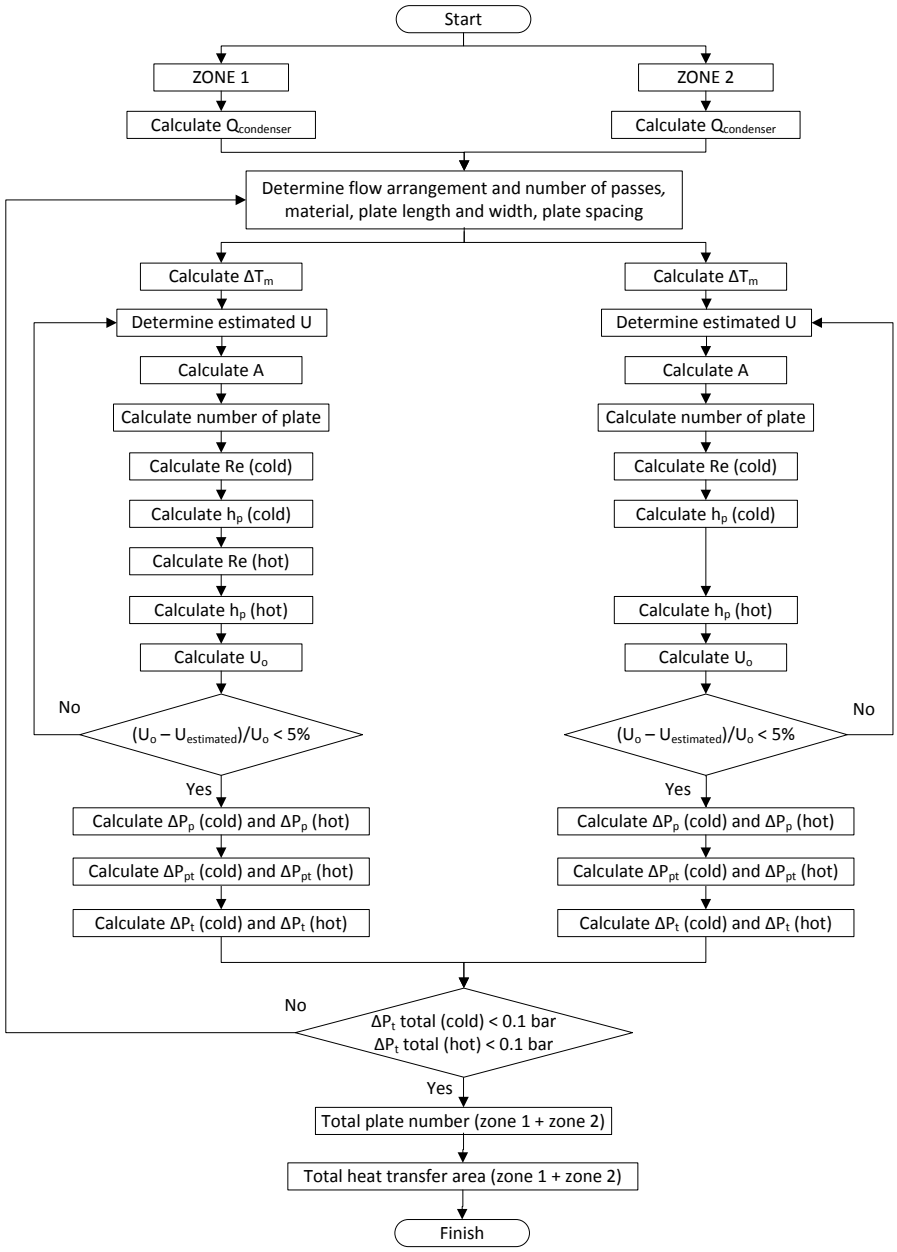

Fig. 3. Design method flow chart of PHE as condenser.

The design was conducted by calculating condenser capacity at both sides and both zones from condenser operating condition in Table 1, determining the constant and independent variables as in Table 2, estimating the overall heat transfer coefficient, and calculating heat transfer area and plate film coefficient. Analysis continued by calculating the overall heat transfer coefficient that has small percent of error with the estimated overall heat transfer coefficient, calculating the pressure drop, the total plate number and the total heat transfer area. The PHE design is based from the method that is explained in [15] and [11].

Table 1. Condenser operating condition.

Operating condition	Hot Side	Cold Side
Fluid	R123	Water
PHE inlet temperature (°C)	62	25
Pressure (bar)	1.545	1
Mass flow rate (kg/hour)	584	2,525

Table 2. The constant and independent variable.

Variable		Assumption
Constant	Flow arrangement	Series, Counter-current
	Number of passes	1:1
	Material plate	Stainless Steel
	Plate thickness (mm), s	0.75
	Plate length (m), L	0.5
	Plate width (m), W	0.125
Independent	Plate spacing (mm), d	2, 3, 4

2.1. Cold side plate (water)

The cooling water heat flow rate in zone 1 and zone 2 is obtained from Equation (1) and (2). The calculation of cooling water plate film coefficient (h_{pc}) for each zone (1 and 2) is described from Equation (3-14).

$$Q_{c\,(cold,\ zone\ 1)} = \dot{m}_c Cp_c (t_2 - t_1^*) \tag{1}$$

$$Q_{c\,(cold,\ zone\ 2)} = \dot{m}_c Cp_c (t_1^* - t_1) \tag{2}$$

where $Q_{c\,(cold,\ zone\ 1)}$ is cold side heat flow rate at zone 1 (kW); $Q_{c\,(cold,\ zone\ 2)}$ is cold side heat flow rate at zone 2 (kW); $\dot{m}_c$ is cooling fluid mass flow rate (kg/s); Cp_c is cooling fluid mass heat capacity (J/kg°C); t_1 is cold fluid temperature, inlet (°C); t_1^* is boundary temperature between zone 1 and 2 (°C); and t_2 is cold fluid temperature, outlet (°C).

$$\Delta T_{lm} = \frac{(T_1 - t_2) - (T_2 - t_1)}{ln\frac{(T_1 - t_2)}{(T_2 - t_1)}} \tag{3}$$

$$\Delta T_m = F_t \Delta T_{lm} \tag{4}$$

$$A = \frac{Q}{U \Delta T_m} \tag{5}$$

$$A_{1p} = LW \tag{6}$$

$$N_p = \frac{A}{A_{1p}} \tag{7}$$

$$N_c = \frac{(N_p - 1)}{2} \tag{8}$$

$$A_f = Wd \tag{9}$$

$$u_p = \frac{\dot{m}_c}{\rho A_f N_c} \tag{10}$$

$$d_e = 2d \tag{11}$$

$$Re = \frac{\rho u_p d_e}{\mu} \tag{12}$$

$$Pr = \frac{C_p \mu}{k_f} \tag{13}$$

$$Nu = \frac{h_p d_e}{k_f} = 0{,}26 Re^{0{,}65} Pr^{0{,}4} \left(\frac{\mu}{\mu_w}\right)^{0{,}14} \tag{14}$$

where ΔT_{lm} is log mean temperature difference (°C); T_1 is hot fluid temperature, inlet (°C); T_2 is hot fluid temperature, outlet (°C); ΔT_m is true temperature difference (°C); F_t is the temperature correction factor; A is heat-transfer area (m^2); U is the overall heat transfer coefficient (W/m^2°C), the initial U value is estimated; A_{1p} is effective area of one plate (m^2); L is effective length (m); W is effective width (m); N_p is number of plates; N_c is number of channel per pass; A_f is channel-cross sectional area (m^2); d is plate spacing (m); u_p is channel velocity (m/s); ρ is fluid density (kg/m^3); d_e is equivalent (hydraulic) diameter (m); Re is Reynold number; and μ is fluid viscosity (kg/m s), Pr is Prandtl number; k_f is fluid thermal conductivity (W/m°C); Nu is Nusselt number; h_p is plate film coefficient (W/m^2°C); and μ_w is fluid viscosity at wall temperature (kg/m s).

2.2. Hot side plate (R123)

The hot fluid heat flow rate in zone 1 and 2 at Equation (15) and (16) are respectively equal with cooling water heat flow rate at Equation (1) and (2) according to the energy balance. The hot fluid plate film coefficient (h_{ph}) zone 1 is calculated from Equation (3-14) and zone 2 is described in Equation (17-19).

$$Q_{h\,(hot,\ zone\ 1)} = \dot{m}_h (h_1 - h_1^*) \tag{15}$$

$$Q_{h\,(hot,\ zone\ 2)} = \dot{m}_h (h_1^* - h_2) \tag{16}$$

where $Q_{h\,(hot,\ zone\ 1)}$ is hot side heat flow rate at zone 1 (kW); $Q_{h\,(hot,\ zone\ 2)}$ is hot side heat flow rate at zone 2 (kW); $\dot{m}_h$ is hot fluid mass flow rate (kg/s); h_1 is hot fluid enthalpy, inlet (J/kg); h_1^* is boundary enthalpy between zone 1 and 2 (J/kg); and h_2 is hot fluid enthalpy, outlet (J/kg).

$$h_c = \left(\frac{1}{U} - \frac{1}{h_{pc}} - \frac{s}{k_p}\right)^{-1} \tag{17}$$

$$t_{sat} - t_{wall} = \frac{U \Delta T_{lm} F_t}{h_c} \tag{18}$$

$$h_p = 0{,}943. \left[\frac{\rho_L (\rho_L - \rho_G) g . H_{LG} k_L^3}{\mu_L . L (t_{sat} - t_{wall})}\right]^{0{,}25} \tag{19}$$

where h_c is condensation heat transfer coefficient (W/m^2°C); h_{pc} is cold-side heat transfer coefficient (W/m^2°C); s is plate thickness (m); k_p is plate thermal conductivity (W/m°C); t_{sat} is saturation temperature (°C); t_{wall} is wall temperature (°C); ρ_L is liquid density (kg/m^3); ρ_G is gas density (kg/m^3); g is gravitational acceleration (m/s^2); H_{LG} is latent heat (J/kg); k_L is liquid thermal conductivity (W/m°C); and μ_L is liquid viscosity (kg/m s).

2.3. Overall coefficient (U_o)

The overall coefficient for each zone (1 and 2) is obtained from Equation (20). Where U_o is the overall coefficient (W/m^2°C); h_{fh} is hot fluid fouling factor coefficient (W/m^2°C); and h_{fc} is cold fluid fouling factor coefficient (W/m^2°C). The initial U value in Equation (5) is continuously estimated until the difference of the estimated U and the result of U_o in Equation (20) has a small percent of error.

$$\frac{1}{U_o} = \frac{1}{h_{ph}} + \frac{1}{h_{fh}} + \frac{s}{k_p} + \frac{1}{h_{pc}} + \frac{1}{h_{fc}} \tag{20}$$

2.4. Total pressure drop (ΔP_t)

The total pressure drop for each side (hot and cold) is described in Equation (21-26). Where j_f is friction factor; ΔP_p is plate pressure drop (bar); L_p is path length (m); u_{pt} is the velocity through the ports (m/s); $\dot{m}$ is mass flow through the ports (kg/s); A_p is area of the port (m^2); d_{pt} is port diameter (m); N_{ps} is number of passes; ΔP_{pt} is pressure loss through the port (bar); and ΔP_t is total pressure drop (bar).

$$j_f = 0.6\, Re^{-0.3} \tag{21}$$

$$\Delta P_p = 8 j_f \left(L_p / d_e\right) \frac{\rho u_p^2}{2} \tag{22}$$

$$u_{pt} = \frac{\dot{m}}{\rho A_p} \tag{23}$$

$$A_p = \frac{\pi d_{pt}^2}{4} \tag{24}$$

$$\Delta P_{pt} = 1.3 \frac{(\rho u_{pt}^2)}{2} N_{ps} \tag{25}$$

$$\Delta P_t = \Delta P_p + \Delta P_{pt} \tag{26}$$

2.5. Total heat transfer area (A_t)

The total heat transfer area is calculated from Equation (27-28). Where $N_{p\,(total)}$ is total number of plates; and A_t is total heat transfer area (m^2).

$$N_{p\,(total)} = N_{p\,(zone\,1)} + N_{p\,(zone\,2)} \tag{27}$$

$$A_t = N_{p\,(total)} A_{1p} \tag{28}$$

3. Result and discussion

The PHE design calculation result in Table 3 shows that the total heat transfer area and the total number of plates increase in the rise of plate spacing, but otherwise the cold fluid total pressure drop and the hot fluid total pressure drop decrease in the rise of plate spacing. These results affirm the previous research result in [11]. These results also can be analyzed with observing the impact sequence of plate spacing parameter to the other calculation result data in Fig. 4a, 4b, 5, 6, 7, 8, 9a, 9b, 10a, and 10b.

Fig. 4a and 4b show that the rises of plate spacing increase the total heat transfer area in both Zone 1 and 2. Due to the increasing total heat transfer area and the constant effective area of one plate, the number of plates in both

Zone 1 and 2 go up. Thus make the number of channel in Zone 1 and 2 rise, except the number of channels in Zone 1 (Fig. 4a) at plate spacing 2 and 3 mm have the same value, because them are the round numbers.

Table 3. PHE design calculation result.

Plate spacing (mm)	2	3	4
Total heat transfer area (m^2)	4.875	5.3125	6.0625
Total number of plates	78	85	97
Cold fluid total pressure drop (bar)	0.407	0.121	0.011
Hot fluid total pressure drop (bar)	1.045	0.309	0.028

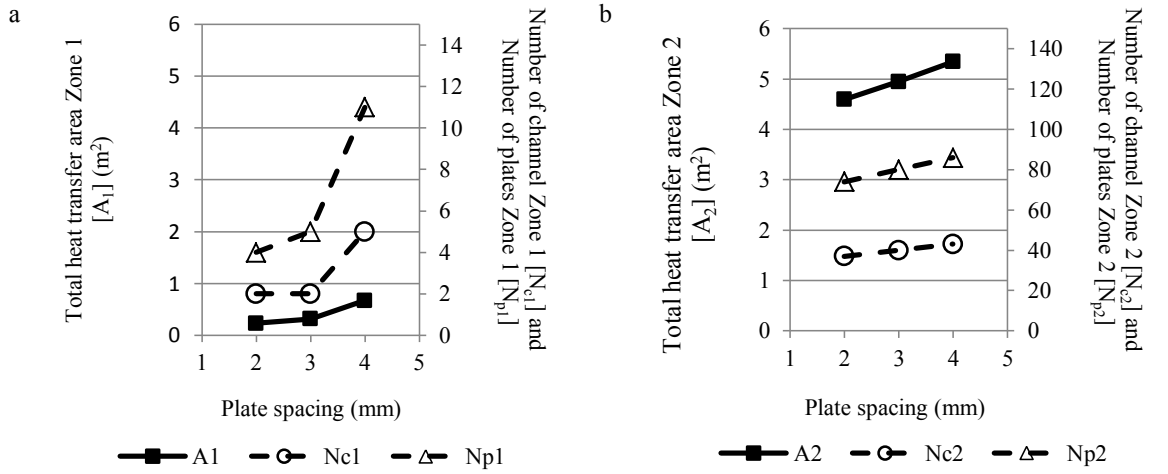

Fig. 4. (a) Effect of plate spacing (d) on number of channel (N_c), number of plates (N_p),and total heat transfer area (A) at Zone 1; (b) Effect of plate spacing (d) on number of channel (N_c), number of plates (N_p),and total heat transfer area (A) at Zone 2.

The methods to calculate plate film coefficient of Zone 1 (cold side and hot side) and Zone 2 (cold side) as in Fig. 9a and Fig. 9b are same and the results can be analyzed as follow. The rises of plate spacing also impact to the enhancement of the channel cross sectional area such in Fig. 5. The increasing of channel cross sectional area and number of channel make the channel velocities in Fig. 5 and Fig. 6 drop, since the fluid mass flow rate and the fluid density are unchanged. When fluid density and fluid viscosity are constant, the decreasing of channel velocity and slight increasing of equivalent diameter (as in Fig. 7) make Reynold numbers in Fig. 7 and Fig. 8 drop, except the Reynold number of Zone 1 (cold side and hot side) in Fig. 7 at plate spacing 2 and 3 mm have the same value, because the multiplication result between their channel velocities and equivalent diameters have the same values. The sharp drop of Reynold number and slight increasing of equivalent diameter at constant Prandtl number and constant fluid thermal conductivity result the decreasing of plate film coefficient in Zone 1 (cold side and hot side) and Zone 2 (cold side). The decreasing of plate film coefficient in Zone 1 (cold side and hot side) at constant fouling factor coefficient (cold fluid and hot fluid), plate thickness, and plate thermal conductivity, result the decreasing of Zone 1 overall coefficient as in Fig. 9a. The decreasing of Zone 1 overall coefficient at constant Zone 1 heat flow rate and true temperature difference, make the Zone 1 total heat transfer area in Fig. 4a increase.

The calculation method of Zone 2 hot side plate film coefficient is different, because there are two phase changed in it. Based on Fig. 9b, the Zone 2 hot side plate film coefficients are almost constant, because they are slight increasing and can be analyzed as follow. The decreasing Zone 2 overall coefficient and cold side plate film coefficient, the unchanged plate thickness and plate thermal conductivity, result the slight increasing of the condensation heat transfer coefficient as in Fig. 6. The sharp drop of Zone 2 overall coefficient and slight increasing of condensation heat transfer coefficient at the constant log mean temperature difference and temperature correction

factor, make the differences between saturated and wall temperature decrease slightly in Fig. 8. Slight drop of the differences between saturated and wall temperature at the unchanged liquid and gas density, gravitational acceleration, latent heat, liquid thermal conductivity, and liquid viscosity, result the slight increasing of Zone 2 hot side plate film coefficient. The slight increasing of Zone 2 hot side plate film coefficient and the decreasing of Zone 2 cold side plate film coefficient at constant fouling factor coefficient (cold fluid and hot fluid), plate thickness, and plate thermal conductivity, result the decreasing of Zone 2 overall coefficient as in Fig. 9b. The decreasing of Zone 2 overall coefficient at the unchanged Zone 2 heat flow rate and true temperature difference, make the Zone 2 total heat transfer area in Fig. 4b increase. The increasing of the Zone 1 total heat transfer area in Fig. 4a and the Zone 2 total heat transfer area in Fig. 4b make the total heat transfer area and the total number of plates in Table 3 increase at the rises of plate spacing.

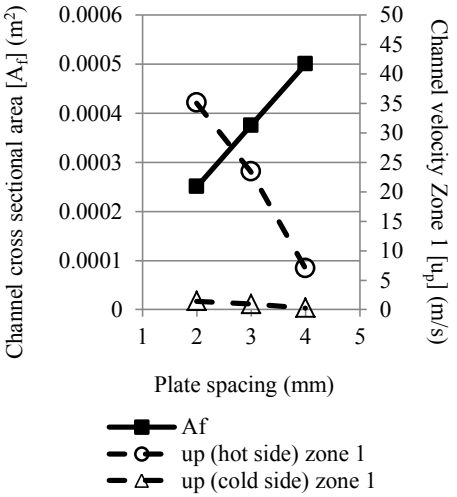

Fig. 5. Effect of plate spacing (d) on channel cross sectional area (A_f) and channel velocity (u_p) Zone 1.

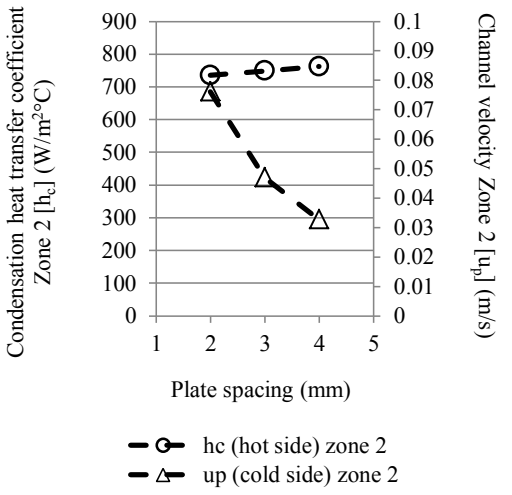

Fig. 6. Effect of plate spacing (d) on condensation heat transfer coefficient (h_c)and channel velocity (u_p) Zone 2.

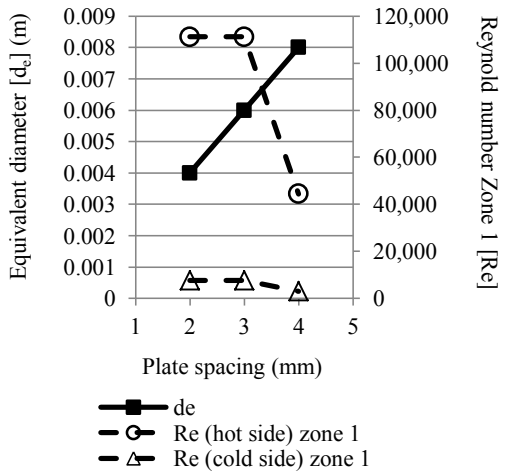

Fig. 7. Effect of plate spacing (d) on equivalent diameter (d_e), and Reynold number (Re) of hot side and cold side at Zone 1.

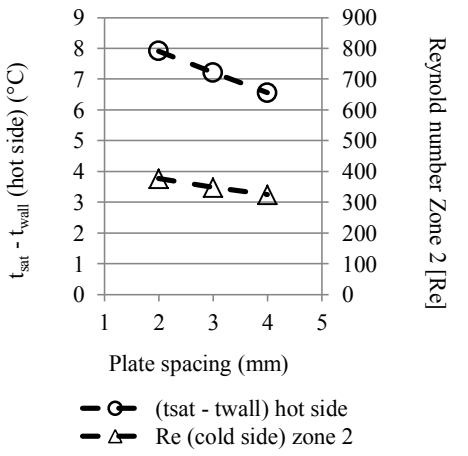

Fig. 8. Effect of plate spacing (d) on the difference between saturated and wall temperature (t_{sat}-t_{wall}) and Reynold number (Re) of cold side at Zone 2.

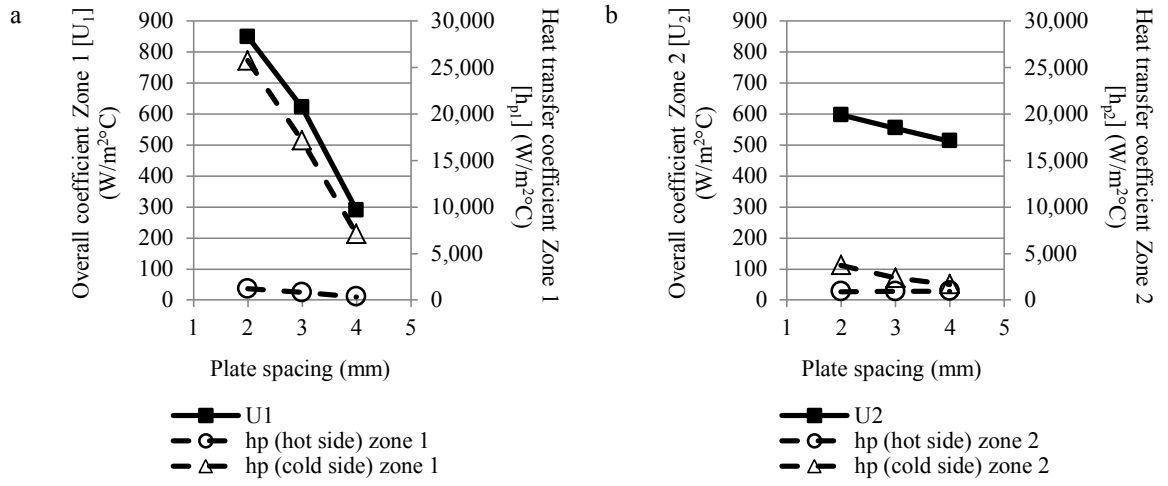

Fig. 9. (a) Effect of plate spacing (d) on the heat transfer coefficient of hot side (h_{ph}) and cold side (h_{pc}), and the overall coefficient (U) at Zone 1; (b) Effect of plate spacing (d) on the heat transfer coefficient of hot side (h_{ph}) and cold side (h_{pc}), and the overall coefficient (U) at Zone 1.

The port diameters are same in the rises of plate spacing, so the areas of the port are unchanged. When the mass flow through the ports, fluid density, and the areas of the port are constant, that conditions result the unchanged of velocity through the ports. Since the fluid density, the velocity through the ports and number of passes are constant, so the pressure losses through the port of cold and hot fluid in Zone 1 and Zone 2 are unchanged in the rises of plate spacing.

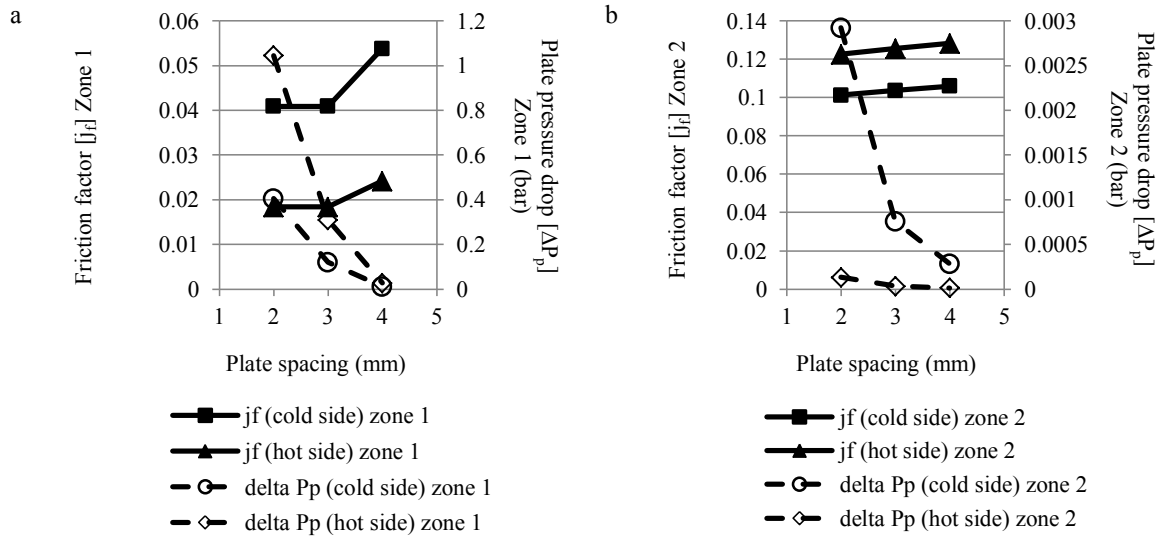

Fig. 10. (a) Effect of plate spacing (d) on the friction factor of hot side (j_{fh}) and cold side (j_{fc}), and the plate pressure drop of hot side (ΔP_{ph}) and cold side (ΔP_{pc}) at Zone 1; (b) Effect of plate spacing (d) on the friction factor of hot side (j_{fh}) and cold side (j_{fc}), and the plate pressure drop of hot side (ΔP_{ph}) and cold side (ΔP_{pc}) at Zone 2.

The decreasing Reynold number of cold and hot fluid in Zone 1 and Zone 2 increase the friction factor of cold and hot fluid in Zone 1 and Zone 2 as in Fig. 10a and Fig. 10b. The increasing of the friction factor and the

equivalent diameter, the decreasing of channel velocity at constant path length and fluid density make the cold and hot fluid plate pressure drop in Zone 1 and Zone 2 decrease as in Fig. 10a and Fig. 10b. As the result, the decreasing of cold fluid in Zone 1 and Zone 2 at the constant pressure losses through the port of cold fluid in Zone 1 and Zone 2 make cold fluid total pressure drop decrease as in Table 3 at the rises of plate spacing. Same with cold fluid, the decreasing of hot fluid in Zone 1 and Zone 2 at the constant pressure losses through the port of hot fluid in Zone 1 and Zone 2 result the decreasing of hot fluid total pressure drop as in Table 3 at the rises of plate spacing.

4. Conclusion

The rises of plate spacing result the increasing of total heat transfer area and total number of plates (unpreferable), but the rises of plate spacing also result the decreasing of cold and hot fluid total pressure drop (preferable), so the size choice of plate spacing can be adjusted with the requirement of the utilization purpose.

References

[1] Y. Dai, *et al.*, "Parametric optimization and comparative study of organic Rankine cycle (ORC) for low grade waste heat recovery," *Energy Conversion and Management,* vol. 50, pp. 576–582, 2009.

[2] S. Quoilin, *et al.*, "Experimental study and modeling of an Organic Rankine Cycle using scroll expander," *Applied Energy,* vol. 87, pp. 1260–1268, 2010.

[3] W. Li, *et al.*, "Effects of evaporating temperature and internal heat exchanger on organic Rankine cycle," *Applied Thermal Engineering,* vol. 31, pp. 4014-4023, 2011.

[4] M. Bianchi and A. D. Pascale, "Bottoming cycles for electric energy generation: Parametric investigation of available and innovative solutions for the exploitation of low and medium temperature heat sources," *Applied Energy,* vol. 88, pp. 1500–1509, 2011.

[5] S. Quoilin and V. Lemort, "Technological and Economical Survey of Organic Rankine Cycle Systems," presented at the 5th European Conference: Economics and Management of Energy in Industry, Portugal, 2009.

[6] A. I. Papadopoulos, *et al.*, "On the systematic design and selection of optimal working fluids for Organic Rankine Cycles," *Applied Thermal Engineering,* vol. 30, pp. 760–769, 2010.

[7] J. P. Roy, *et al.*, "Performance analysis of an Organic Rankine Cycle with superheating under different heat source temperature conditions," *Applied Energy,* vol. 88, pp. 2995–3004, 2011.

[8] J. Bao and L. Zhao, "A review of working fluid and expander selections for organic Rankine cycle," *Renewable and Sustainable Energy Reviews,* vol. 24, pp. 325–342, 2013.

[9] M. Li, et al., "Construction and preliminary test of a low-temperature regenerative Organic Rankine Cycle (ORC) using R123," Renewable *Energy,* vol. 57, pp. 216-222, 2013.

[10] S. H. Kang, "Design and experimental study of ORC (organic Rankine cycle) and radial turbine using R245fa working fluid," *Energy,* vol. 41, pp. 514-524, 2012.

[11] M. W. Jiangfeng Wang, Maoqing Li, Jiaxi Xia, Yiping Dai, "Multi-objective optimization design of condenser in an organic Rankine cycle for low grade waste heat recovery using evolutionary algorithm," *International Communications in Heat and Mass Transfer,* vol. 45, pp. 47-54, 2013.

[12] L. Wang and B. Sunden, "Optimal design of plate heat exchangers with and without pressure drop specifications," *Applied Thermal Engineering,* vol. 23, pp. 295-311, 2003.

[13] J. Zhu and W. Zhang, "Optimization design of plate heat exchangers (PHE) for geothermal district heating systems," *Geothermics,* vol. 33, pp. 337-347, 2004.

[14] S. Karellas, *et al.*, "Influence of supercritical ORC parameters on plate heat exchanger design," *Applied Thermal Engineering,* vol. 33-34, pp. 70-76, 2012.

[15].R. K. Sinnott, *Chemical Engineering Design*, 4th ed. vol. 6. Oxford: Elsevier Butterworth-Heinemann, 2005.